Title
H. pylori CheZHP and ChePep form a distinct complex

Journal
Molecular Microbiology, 97(6)

ISSN
0950-382X

Authors
Lertsethtakarn, Paphavee
Howitt, Michael R
Castellon, Juan
et al.

Publication Date
2015-09-01

DOI
10.1111/mmi.13086

Peer reviewed

Helicobacter pylori $CheZ_{HP}$ and ChePep form a novel chemotaxis-regulatory complex distinct from the core chemotaxis signaling proteins and the flagellar motor

Paphavee Lertsethtakarn[1,#], Michael R. Howitt[2,##], Juan Castellon[1], Manuel R. Amieva[2], Karen M. Ottemann[1,*]

[1]Department of Microbiology and Environmental Toxicology, University of California, Santa Cruz, Santa Cruz, CA 95064, USA

[2]Department of Microbiology and Immunology, Stanford University School of Medicine, Stanford, CA 94305 USA

[*]Corresponding author: e-mail ottemann@ucsc.edu; Tel (+1) 831 459 3482; Fax (+1) 831 459 3524

[#]Present address: AFRIMS-USAMC 315/6 Rajvithi Road Bangkok, 10400 Thailand

##Present address: Department of Immunology and Infectious Diseases, Harvard School of Public Health, Boston, MA 02115

Abstract

Chemotaxis is important for *Helicobacter pylori* to colonize the stomach. Like other bacteria, *H. pylori* uses chemoreceptors and conserved chemotaxis proteins to phosphorylate the flagellar rotational response regulator, CheY, and modulate the flagellar rotational direction. Phosphorylated CheY is returned to its non-phosphorylated state by phosphatases such as CheZ. In previously studied cases, chemotaxis phosphatases localize to the cellular poles by interactions with either the CheA chemotaxis kinase or flagellar motor proteins. We report here that the *H. pylori* CheZ, $CheZ_{HP}$, localizes to the poles independently of the flagellar motor, CheA, and all typical chemotaxis proteins. Instead, $CheZ_{HP}$ localization depends on the chemotaxis regulatory protein ChePep and reciprocally, ChePep requires $CheZ_{HP}$ for its polar localization. We furthermore show that these proteins interact directly. Functional domain mapping of $CheZ_{HP}$ determined the polar localization motif lies within the central domain of the protein, and that the protein has regions outside of the active site that participate in chemotaxis. Our results suggest that $CheZ_{HP}$ and ChePep form a distinct complex. These results therefore suggest the intriguing idea that some phosphatases localize independently of the other chemotaxis and motility proteins, possibly to confer unique regulation on these proteins' activities.

Introduction

Chemotaxis is the ability to sense external environmental cues and respond by moving toward beneficial situations and away from harmful ones. Bacteria utilize chemotaxis to colonize a variety of habitats, including the mammalian host (Josenhans and Suerbaum, 2002; Miller *et al.*, 2009). Bacterial chemotaxis depends on a set of signal transduction proteins comprised of chemoreceptors and chemotaxis signal transduction proteins (Wadhams and Armitage, 2004). These proteins typically localize to the bacterial pole in a supermolecular cluster with extensive interactions between chemoreceptors and chemotaxis signaling proteins (Sourjik and Armitage, 2010). These interactions serve to amplify small signals, allow integration of multiple chemoreceptors, and provide protein-protein regulatory contacts. To date, all chemotactic microbes examined display clusters of chemotaxis proteins, supporting the importance of this organization (Briegel *et al.*, 2009).

Helicobacter pylori is a motile human gastric pathogen that relies on chemotaxis to colonize mammalian stomachs (Foynes *et al.*, 2000; Terry *et al.*, 2005; Lertsethtakarn *et al.*, 2011). *H. pylori* infection results in ulcers and gastric cancer, and affects millions worldwide (Polk and Peek, 2010; Salama *et al.*, 2013). *H. pylori* swims utilizing a cluster of 3-7 flagella localized to one pole. The chemotaxis signal transduction system of *H. pylori* likely localizes to the flagellar pole, based on studies with many bacteria including the related one, *Helicobacter hepaticus* (Briegel *et al.*, 2009). The composition of the *H. pylori* chemotaxis signal transduction system is comparable to that of the model bacterium *Escherichia coli* (Lertsethtakarn *et al.*, 2011). Both organisms utilize specific chemoreceptors to sense their environments. *H. pylori* has four chemoreceptors—TlpA, TlpB, TlpC and TlpD—that have been reported to sense arginine, bicarbonate (Cerda *et al.*, 2003), pH (Croxen *et al.*, 2006; Sweeney *et al.*, 2012), the quorum sensing mole-

cule, autoinducer-2 (AI-2) (Rader *et al.*, 2011) and energy (Schweinitzer *et al.*, 2008). The receptors transmit ligand-binding information via coupling proteins, CheW or CheV, to the CheA histidine kinase, which is sometimes called CheAY in *H. pylori* because it has a receiver (REC) domain fused at the C-terminus. *H. pylori* possesses more coupling proteins than *E. coli*: one CheW and three CheV proteins. CheV proteins are chimeras of CheW and a phosphorylatable REC domain (Pittman *et al.*, 2001; Lowenthal, Simon, *et al.*, 2009; Alexander *et al.*, 2010). CheAY phosphorylates the response regulator, CheY, which consists of a REC domain (Jiménez-Pearson *et al.*, 2005; Lertsethtakarn and Ottemann, 2010). Phosphorylated CheY (CheY-P) interacts with the flagellar motor to cause clockwise flagellar rotation and bacterial reversals, as opposed to straight swimming when CheY is non-phosphorylated. CheY-P is returned to the non-phosphorylated state by both its own auto-dephosphorylation, as well as the action of phosphatases. In *H. pylori*, the only known phosphatase is CheZ, called $CheZ_{HP}$ in this system.

In addition to the proteins mentioned above, *H. pylori* possesses a chemotaxis protein called ChePep, which is found only in the Epsilon proteobacteria (Howitt *et al.*, 2011). ChePep was previously annotated as a hypothetical poly E-rich protein, and like most of the *H. pylori* chemotaxis genes, is encoded in an operon without other chemotaxis genes. ChePep is critical for efficient chemotaxis (Howitt *et al.*, 2011). ChePep deletion mutants migrate poorly through soft agar, displaying a ~ 25% reduction in soft agar colony diameter (Howitt *et al.*, 2011). Additionally, they display about 11-times greater reversals than wild type, a phenotype that is dependent on CheY. This finding suggests that ChePep is required for the efficient dephosphorylation of CheY-P, similar to $CheZ_{HP}$ (Howitt *et al.*, 2011). ChePep has a preponderance of glutamic acids and an N-terminal REC domain of unknown function, but otherwise contains no recognizable domains. It localizes to the bacterial pole by an as-yet unknown mechanism (Howitt *et al.*, 2011).

Specifically, ChePep is found at only the flagellar pole in short, recently divided cells, and then is seen at both poles as the cells elongate before division (Howitt *et al.*, 2011).

The return of CheY-P to its non-phosphorylated state is a critical aspect of chemotaxis because this action allows the system to reset and the bacteria to respond to new signals. Across different microbes, CheY-P dephosphorylation is promoted by either specific phosphatases or by alternate CheA kinase targets (Wadhams and Armitage, 2004; Silversmith, 2010). The first identified and best-studied chemotaxis phosphatase is CheZ, although there are several other types of phosphatases, including CheC, FliY, and CheX that all share mechanisms similar to that of CheZ (Hess *et al.*, 1988; Zhao *et al.*, 2002; Silversmith, 2010). Regardless of the exact phosphatase, phosphatase activity is generally restricted to one cellular location to prevent formation of a CheY-P gradient throughout the cell (Rao *et al.*, 2005; Lipkow, 2006). This localization, in turn, allows all flagellar complexes—spread throughout the cell in the peritrichously flagellated *E. coli*—to receive the same signal and therefore rotate all motors in the same direction. In support of this idea, CheZ and CheC are localized to the chemotaxis signaling complex while another phosphatase, FliY, localizes to the flagellar motor (Rao *et al.*, 2005). *E. coli* CheZ localizes to the chemotaxis cluster via an interaction with both CheA and a variant of CheA called CheA short (CheAs) that results from internal translation initiation (Wang and Matsumura, 1996; Cantwell *et al.*, 2003; Kentner and Sourjik, 2009). This form of CheA lacks the first 97 amino acids, a truncation that enhances a weak full-length CheA-CheZ interaction. FliY, on the other hand, appears to localize via interactions with the FliM and FliN components of the flagellar motor (Szurmant *et al.*, 2003). These studies thus show that phosphatases localize at either the input of the chemotaxis system (the chemotaxis signaling complex), or to the output at the flagellar motor.

H. pylori relies on a $CheZ_{HP}$ for CheY-P dephosphorylation, but CheZ proteins share only small regions of homology when compared across different bacterial families, making it difficult to identify them and define functional regions (Terry *et al.*, 2006; Wuichet *et al.*, 2007; Lertsethtakarn and Ottemann, 2010). The main region of homology between different CheZ proteins is located in the C-terminal half. This region contains the active site aspartate and glutamine (D143/189 and Q147/193 in *E. coli* CheZ and $CheZ_{HP}$, respectively) and a CheY-P binding peptide within the last 12 amino acids (Fig. 1A). Lertsethtakarn and Ottemann used purified $CheZ_{HP}$ in several *in vitro* assays to determine that the protein has phosphatase activity that was dependent on D189, Q193, and the C-terminal 12 amino acids, suggesting it used the same mechanism as *E. coli* CheZ (Lertsethtakarn and Ottemann, 2010). $CheZ_{HP}$ was able to dephosphorylate CheY-P as *E. coli* CheZ does, but additionally dephosphorylated the REC-domain proteins CheV2 and CheAY (Lertsethtakarn and Ottemann, 2010). While the C-terminal half of $CheZ_{HP}$ is moderately conserved, the N-terminal 140 amino acids of $CheZ_{HP}$ shows low amino acid homology with *E. coli* CheZ (Terry *et al.*, 2006; Lertsethtakarn and Ottemann, 2010), suggesting that the functions of this region may not be conserved. Of note, this region is longer by approximately 30 amino acids as compared to *E. coli*'s, and bears multiple repeats of lysine and glutamic acid, making the protein very charged (Fig. 1A). In *E. coli* CheZ, increased phosphatase activity gain of function mutations all map to the N-terminal region (Sanna and Simon, 1996). Located within this N-terminal region, specifically amino acids 70-133, is the portion of *E. coli* CheZ that is required for interaction with CheAs and subcellular localization (Cantwell *et al.*, 2003).

Due to the poor conservation of $CheZ_{HP}$ in general, we questioned whether $CheZ_{HP}$ would localize to the chemotaxis signaling cluster. To place $CheZ_{HP}$ cellular localization in the context of *H. pylori* chemotaxis system, we also determined the cellular localization of *H. pylori*

core chemotaxis proteins. We found that $CheZ_{HP}$ localizes to the bacterial pole as do other *H. pylori* chemotaxis signaling proteins, but surprisingly, $CheZ_{HP}$ polar localization is independent of known chemotaxis and flagellar-related proteins. Instead, $CheZ_{HP}$ polar localization depends on the chemotaxis regulatory protein, ChePep (Howitt *et al.*, 2011). ChePep localization furthermore depends on $CheZ_{HP}$. Functional domain mapping of $CheZ_{HP}$ determined the polar localization motif lies within the central domain of the protein, and that the protein has regions outside of the active site that contribute to chemotactic function. This unexpected localization pattern of $CheZ_{HP}$ and ChePep suggest that they form a protein complex that is distinct from the chemoreceptors and flagellar motor, suggesting that *H. pylori* localizes its phosphatase not at the input or output of chemotaxis as do other known phosphatases, but at a third location.

Results

$CheZ_{HP}$ controls swimming reversals and possesses multiple functional regions

In vitro, $CheZ_{HP}$ has been demonstrated to dephosphorylate CheY-P, as expected for a CheY phosphatase (Lertsethtakarn and Ottemann, 2010). Its reported *in vivo* behavior, however, did not match this activity: *$cheZ_{HP}$* mutants were shown to be straight swimming-biased by Terry *et al*., instead of the predicted hyper-reversal behavior associated with elevated CheY-P (Terry *et al.*, 2006). The *$cheZ_{HP}$* allele used by Terry *et al*. was a partial deletion mutant that replaced the majority of *$cheZ_{HP}$* with a *cat* gene, but retained coding potential for CheZ amino acids 1-13 and 239-253 (Fig. 1A) (Terry *et al.*, 2006). The N-terminal peptide has no known function or homology, but the C-terminal region of CheZ contains a conserved CheY-P binding sequence within the last 12 amino acids (Blat and Eisenbach, 1996; Lertsethtakarn and Ottemann, 2010). We hypothesized that these regions might affect *H. pylori* chemotactic ability, possibly via interactions

with other chemotaxis proteins, so we first set out to create a complete *cheZ*$_{HP}$ deletion, and to analyze possible roles of other regions of CheZ$_{HP}$.

cheZ$_{HP}$ mutants were created by replacing the endogenous chromosomal copy of *cheZ*$_{HP}$ with various mutant alleles, creating unmarked mutations that were under wild-type *cheZ*$_{HP}$ transcriptional control. Deletion of the entire *cheZ*$_{HP}$ coding region (*ΔcheZ*$_{HP}$) resulted in a strain that migrated poorly through Brucella Broth-FBS soft agar, with a similar degree of defect as other fully non-chemotactic strains such as a full deletion of *cheW* (Fig. 1B). When a wild-type copy of *cheZ*$_{HP}$ was introduced back into the original locus (complement), soft agar migration ability was restored to levels that were equivalent to wild type, supporting that the *cheZ*$_{HP}$ mutation caused the soft agar chemotaxis phenotype (Fig. 1B). The original *cheZ*$_{HP}$ mutant (Δ*cheZ*$_{HP}$*::cat*), which retained CheZ$_{HP}$ amino acids 1-13 and 239-253, was able to migrate somewhat better in the soft agar assay as compared to the *ΔcheZ*$_{HP}$ strain (Fig. 1B).

We next examined the swim behavior of the complete *cheZ*$_{HP}$ deletion (Δ*cheZ*$_{HP}$). We filmed swimming *H. pylori* and counted the number of direction switches over a five second swim period. Using this method, we found that wild-type *H. pylori* displayed approximately two direction changes in five seconds (21.6 per minute), while the Δ*cheZ*$_{HP}$ mutant had a statistically significant 2-fold increase in the number of direction changes (4 per five seconds or 48 per minute) (Fig. 2). As described before, strains bearing the Δ*cheZ*$_{HP}$::*cat* allele almost never changed direction (Fig. 2). These results suggest several things. First, the original Δ*cheZ*$_{HP}$::*cat* allele is not a null allele, while the full deletion (Δ*cheZ*$_{HP}$) is. Second, loss of *cheZ*$_{HP}$ leads to elevated CheY-P, based on the increase in bacterial reversals. Third, the regions of CheZ$_{HP}$ retained in the Δc*heZ*$_{HP}$::*cat* allele retain some ability to function in the chemotaxis pathway. Specifically,

they enhance chemotactic migration and promote straight swimming behavior, possibly via an actual function or ability to interact with particular chemotaxis proteins.

We then expanded our analysis to explore additional $CheZ_{HP}$ alleles. $CheZ_{HP}$ conserves two main regions compared to *E. coli* CheZ, both of which were shown experimentally to be required for phosphatase activity *in vitro* (Lertsethtakarn and Ottemann, 2010): the region including the active site residues of D189 and Q193, and the 12 amino acid C-terminal CheY-P binding region ($CheZ_{HP}$ 241-253) (Fig. 1A). Mutants that altered the $CheZ_{HP}$ active site (D189N or Q193R) created strains that behaved similar to *che*Z_{HP} null mutants: they displayed hyper-reversal behavior (Fig. 2), and migrated poorly through the soft agar (Fig. 1B), although not as poorly as complete nulls. Combining these findings with previous *in vitro* work that showed that $CheZ_{HP}$ D189N and Q193R lose phosphatase activity (Lertsethtakarn and Ottemann, 2010), suggests that these mutants lose phosphatase activity *in vivo*, but retain some function, perhaps in interactions with other parts of the chemotaxis signaling pathway that enhance soft agar migration.

To further home in on the regions of $CheZ_{HP}$ that promote chemotactic function, we analyzed the soft-agar phenotypes of several additional truncated mutants. These included a variant that removed the 39 amino acids at the N-terminus ($CheZ_{HP}$ ΔN_{39}), the last 12 amino acids (CheZ ΔC_{12}), one that retained only the first 39 amino acids ($CheZ_{HP}$ N-only), and one that retained only the last 12 amino acids ($CheZ_{HP}$ C-only). Interestingly, each of these strains was able to migrate better than a strain with the Δ*che*Z_{HP} null allele, although all were defective compared to wild type (Fig. 1B). Overall, these results are consistent with the idea that both the N and C terminal regions of $CheZ_{HP}$ contribute to *H. pylori*'s overall chemotactic ability.

H. pylori core chemotaxis proteins form a polar cluster

Based on the lack of conservation between $CheZ_{HP}$ and *E. coli* CheZ, we were interested in whether $CheZ_{HP}$ would localize to the chemotaxis signaling cluster as does *E. coli* CheZ (Cantwell *et al.*, 2003). To determine protein location, we used immunofluorescence with antibodies specific to each protein. Of note, this approach allowed us to use native proteins expressed at wild-type levels, as opposed to fusion or overexpressed proteins. First, we determined the location of proteins of the *H. pylori* chemotaxis signaling cluster, by examining the location of two core signaling proteins, CheAY and CheV1. Each of these proteins was polar, with protein detected at either one or both poles (Fig. 3). This distribution is likely due to the age of the cells, with recently-divided cells having proteins at only the flagellated pole and older cells having proteins localized at both poles, as documented previously for the *H. pylori* chemotaxis protein ChePep (Howitt *et al.*, 2011) as well as *E. coli* chemotaxis proteins (Ping *et al.*, 2008). The chemoreceptors similarly localized to the poles, although some cytoplasmic staining could also be seen (Fig. 3). Control reactions with *H. pylori* strains lacking the proteins under study confirmed that each antibody was specific (Fig. 3). We next assessed whether these proteins were part of a supermolecular cluster anchored by the chemoreceptors, by observing localization in a mutant that lacks all of the chemoreceptors (ΔTlpABCD). As predicted for a chemoreceptor-anchored cluster, CheAY and CheV1 lost their polar localization in the absence of the chemoreceptors, and instead distribute throughout the cell in a punctate or clustered pattern (Fig. 3). These results together suggest that *H. pylori* chemotaxis signaling proteins reside in a polar cluster that is anchored by the chemoreceptor proteins, in an organization similar to that seen in other bacterial species, including close relatives of *H. pylori* (Briegel *et al.*, 2009).

H. pylori CheZ forms a polar cluster that does not depend on the chemotaxis proteins

We next examined the localization of $CheZ_{HP}$. As found with the chemoreceptors and core signaling proteins, $CheZ_{HP}$ localized to either one or both cellular poles (Fig. 4A and Table 1). Surprisingly, deletion of the chemoreceptors did not alter the polar position of $CheZ_{HP}$ (Fig. 4B, Table 1), as it had for CheAY and CheV1 (Fig. 3). We then tested $CheZ_{HP}$ localization in mutants lacking each of the chemotaxis signaling proteins. We were particularly interested in CheAY, as the *E. coli* ortholog of this protein recruits *E. coli* CheZ to the chemoreceptor complex (Cantwell *et al.*, 2003), although *H. pylori* does not have a detectable CheA-short form by immunoblotting (data not shown). Again $CheZ_{HP}$ remained polar even without CheAY (Fig. 4B, Table 1). We then analyzed $CheZ_{HP}$ localization in mutants lacking each additional known chemotaxis signal transduction protein (CheV1, CheV2, CheV3, CheW, CheV1CheV2 double mutant and CheY). $CheZ_{HP}$ polar localization was not affected by the removal of any of these chemotaxis proteins (Fig. 4B, Table 1).

$CheZ_{HP}$ forms a polar cluster that does not depend on flagellar proteins

We expanded our search for proteins that anchor $CheZ_{HP}$ to the pole to examine components of the flagellar motor (FliG, FliM, FliN, FliY) (Lowenthal, Hill, *et al.*, 2009), the MS ring (FliF) (Allan *et al.*, 2000), and the motor (MotB) (Ottemann and Lowenthal, 2002). Each of these single mutants retained $CheZ_{HP}$ at the pole suggesting none were singly responsible for $CheZ_{HP}$ polar localization (Fig. 4C, Table 1). We speculated that perhaps several proteins were sufficient for $CheZ_{HP}$ polar localization, so we examined mutants that were missing the flagellar transcriptional regulators and thus lack several flagellar-related proteins. Specifically, we analyzed mutants lacking FlhA and FlhF, which are the master regulators for intermediate and late flagellar

biosynthesis genes as well as several non-flagellar genes (Niehus *et al.*, 2004). We also analyzed mutants lacking FliA/ σ^{28}, which regulates several intermediate and late flagellar genes including flagellin (*flaA* and *flaB*), *flgE1* (hook), along with non-flagellar genes *envA*, and *omp11* (Niehus *et al.*, 2004). None of these mutations resulted in loss of $CheZ_{HP}$ from the pole (Fig. 4C, Table 1). Similar results were obtained with the *flhG* mutant, which encodes a protein that regulates flagellar number and placement (Kazmierczak and Hendrixson, 2013), as well as HP0062, the only protein suggested to interact with $CheZ_{HP}$ based solely on a genome-wide two hybrid analysis (Rain *et al.*, 2001) (Table 1). We thus concluded that $CheZ_{HP}$ is not anchored at the pole via known chemotaxis or flagellar proteins.

$CheZ_{HP}$ and ChePep depend on each other for polar localization

We next turned our attention to ChePep (Howitt *et al.*, 2011). Cells lacking ChePep switch direction frequently (Howitt *et al.*, 2011), as do $CheZ_{HP}$ mutants (Fig. 2). ChePep was previously observed to localize to the bacterial pole (Howitt *et al.*, 2011) (Fig. 4A), but the protein components required for its localization were not known. We therefore examined whether ChePep required the chemotaxis signaling or flagella proteins. Similar to what was observed for $CheZ_{HP}$, we found that ChePep localizes to the poles independently of the chemotaxis signaling complex and the flagella (Fig. 4B-C, Table 1). Because ChePep and $CheZ_{HP}$ displayed similar localization patterns, we therefore examined whether loss of ChePep would affect $CheZ_{HP}$. We found that $CheZ_{HP}$ polar localization was substantially different from wild type in the Δ*chePep* mutant background (Fig. 4D, Table 1). In particular, we found that a substantial fraction of $CheZ_{HP}$ was lost from the pole, and a new population appeared either laterally dispersed or diffuse throughout the cell (Fig. 4C, Table 1, Supplemental movie 1). Control experiments con-

firmed that loss of either *cheZ* or *chePep* did not affect the expression of the other (Fig. 5). Furthermore, $CheZ_{HP}$ localization could be restored by complementing ChePep *in trans* (Fig. 4D and Supplemental movie 1).

We next examined whether ChePep localization would depend on $CheZ_{HP}$. In mutants lacking $CheZ_{HP}$, ChePep no longer tightly localized to the poles and was found along the length of the bacteria organized in what appears to be a helical conformation (Fig. 4D, Table 1, Supplemental Movie 1). Together, these findings indicate that $CheZ_{HP}$ and ChePep depend on each other for their polar localization and form a novel chemotaxis protein cluster distinct from the flagellar or chemotaxis signaling complexes.

The $CheZ_{HP}$ localization region maps to amino acids 40-229

To gain additional insight into the localization requirements of $CheZ_{HP}$ and ChePep, we analyzed the $CheZ_{HP}$ truncated mutants that lacked either the first 39 amino acids ($CheZ_{HP}\,\Delta N_{39}$) or the last 12 amino acids $CheZ_{HP}\,\Delta C_{12}$). Both of these truncated variants produced protein that was detected by our anti-$CheZ_{HP}$ polyclonal antibody (Fig. 6). In contrast the small $CheZ_{HP}$ pieces of $CheZ_{HP}$ N-only or $CheZ_{HP}$ C-only were not detected by our antibodies, so were not analyzed further. Immunofluorescence analysis of whole *H. pylori* showed that both of these $CheZ_{HP}\,\Delta N_{39}$ and $CheZ_{HP}\,\Delta C_{12}$ localized to the pole in a manner that was indistinguishable from that of full-length $CheZ_{HP}$, suggesting they retain folding requirements for this function (Fig. 6, Table 1). Additionally, ChePep localization was not affected by deletion of either the $CheZ_{HP}$ N or C terminus (Fig. 6, Table 1). These results suggest that region responsible for polar localization of $CheZ_{HP}$ maps to the middle of $CheZ_{HP}$, corresponding to amino acids 40-241.

$CheZ_{HP}$ and ChePep interact directly

Our results suggest that $CheZ_{HP}$ and ChePep form a distinct chemotaxis-regulatory complex, so we next examined whether they interact directly. We used co-immunoprecipitation with purified proteins (Fig. 7A), and found that $CheZ_{HP}$ was co-immunoprecipitated with ChePep, suggesting these proteins interact directly (Fig.7B), and ChePep was similarly co-immunoprecipitated with $CheZ_{HP}$ (data not shown). Neither $CheZ_{HP}$ nor ChePep have predicted transmembrane domains, but both were not detergent soluble as most cytoplasmic proteins, e.g. CheY, are (Fig. 5). Solubility did not change in the presence or absence of either protein (Fig. 5). All together, these findings suggest that $CheZ_{HP}$ and ChePep and are poorly soluble.

Discussion

In this manuscript, we report that the *H. pylori* CheZ phosphatase ($CheZ_{HP}$) localizes to the bacterial pole as do other phosphatases, but its localization relies on unique interactions. The other *H. pylori* chemotaxis proteins are also polar, as shown previously for ChePep (Howitt *et al.*, 2011). Unexpectedly, $CheZ_{HP}$ localization does not depend on the chemoreceptors or CheA, as would be expected from the *E. coli* paradigm, or on any flagellar proteins, as one would predict from other chemotaxis phosphatases (Rao *et al.*, 2005). Instead, $CheZ_{HP}$ localization depends on the ChePep chemotaxis protein (Howitt *et al.*, 2011) and conversely ChePep localization depends on $CheZ_{HP}$. This finding raises the intriguing possibility that some phosphatases, including $CheZ_{HP}$ and ChePep, exist in a complex that is distinct from the core chemotaxis signaling and flagellar complexes. We also show that $CheZ_{HP}$ behaves as a phosphatase *in vivo*, based on the reversal-biased behavior of a *che*Z_{HP} null mutant. This outcome agrees with previous biochemical analysis (Lertsethtakarn and Ottemann, 2010). Somewhat surprisingly, we found that $CheZ_{HP}$ regions outside of the known phosphatase active site and CheY-P binding regions play a role in chemotactic soft agar migration. This finding suggests that these regions retain some function that is not strictly related to phosphatase activity.

$CheZ_{HP}$ localization depends on ChePep, a protein that functions in the chemotaxis pathway and is found only in Epsilon Protebacteria. ChePep and $CheZ_{HP}$ are similar in many ways: as we show here, both localize to the pole, and null mutants of either show hyper-reversal phenotypes (Howitt *et al.*, 2011). Both are highly negatively charged with acidic isoelectric points of 4.29 and 4.63, respectively. The fact that both ChePep and $CheZ_{HP}$ mutants display hyper reversals suggests that loss of either protein creates elevated CheY-P. One possible explanation for this phenotype is that loss of a ChePep-$CheZ_{HP}$ interactions results in less active $CheZ_{HP}$. Our

data showing that $CheZ_{HP}$ and ChePep interact directly supports this idea. Protein-protein interactions are known to activate *E. coli* CheZ; specifically, interactions with CheA-short activate CheZ 2.5-fold (Wang and Matsumura, 1996; Cantwell and Manson, 2009). ChePep contains a REC domain (Howitt *et al.*, 2011) —a type of domain that normally interacts with CheZ. Thus one possibility is that ChePep uses its REC domain to bind $CheZ_{HP}$ and enhances its activity. Another possibility is that without ChePep, $CheZ_{HP}$ is mislocalized and chemotaxis is inefficient in this situation, as discussed below. A third possibility is that both $CheZ_{HP}$ and ChePep have phosphatase activity. Preliminary *in vitro* experiments, however, did not detect any phosphatase activity associated with ChePep (data not shown). A discrete $CheZ_{HP}$ localization was expected, given that other chemotaxis phosphatases localize to specific cellular sites (Rao *et al.*, 2005; Lipkow, 2006). Computer models suggest that phosphatase localization prevents formation of a CheY-P gradient throughout the cell, which in turn allows all flagellar complexes to receive the same signal, rotate their motors in cooperation, and confer efficient cell migration (Rao *et al.*, 2005; Lipkow, 2006). Unexpectedly, $CheZ_{HP}$ localization did not depend on the chemoreceptors, CheAY, other chemotaxis proteins, or flagellar proteins. Thus the localization mechanism of $CheZ_{HP}$ differs from that of *E. coli* CheZ, which depends on CheA and the chemoreceptors (Cantwell *et al.*, 2003), and FliY, which depends on other flagellar motor proteins (Szurmant *et al.*, 2003). Instead, its localization depends on the chemotaxis protein ChePep. Conversely, ChePep localization depends on $CheZ_{HP}$. Thus it appears that each of these proteins enhances the polar localization of the other, by an as-yet-unknown mechanism.

An additional finding reported here is that *H. pylori* chemoreceptors form a polar cluster that includes the core signaling proteins CheAY and CheV1, and presumably others. When the chemoreceptors are absent, CheAY and CheV1 are no longer polar (Fig. 3). Instead, they appear

in the cytoplasm in manner that is clearly non-polar , but does retain some punctate aspects for as yet unknown reasons. This finding is not surprising, given that all bacteria analyzed have a polar chemoreceptor supermolecular cluster (Briegel *et al.*, 2009). *H. pylori* had not been specifically analyzed, although the related microbe *Helicobacter hepaticus* had been. In *H. hepaticus*, the chemoreceptor cluster forms at the pole that also contains the flagella (Briegel *et al.*, 2009). The core chemotaxis signaling cluster of *H. pylori* also appears to form at the flagellar pole in recently-divided cells, and then forms at the second pole prior to cell division (Howitt *et al.*, 2011). We additionally observed minor cytoplasmic or lateral chemoreceptor distribution, as has been observed in *E. coli*, suggesting that both polar and lateral clusters might occur (Maddock and Shapiro, 1993; Greenfield *et al.*, 2009).

The finding that $CheZ_{HP}$ and ChePep localize independently of the two other motility related complexes—the core chemotaxis complex and flagellar basal body— suggests that they may form a third chemotaxis complex. The reason behind this distinct localization is not yet known. However, it should be pointed out that both *E. coli* and *B. subtilis* have polar chemotaxis proteins and peritrichous flagella, while *H. pylori* has chemotaxis and flagella at one pole. No other phosphatases from polarly flagellated bacteria have been analyzed. One possibility is that the $CheZ_{HP}$-ChePep complex is under a distinct regulatory control that is afforded by its separation from the other motility-related complexes. ChePep is found only in the Epsilon proteobacteria, suggesting this Class of bacteria may have evolved unique regulatory mechanisms.

The characterization of various $cheZ_{HP}$ mutants uncovered that portions of $CheZ_{HP}$ without any known phosphatase activity modulate chemotaxis. Strains completely lacking $cheZ_{HP}$ had reduced migration in the soft agar assay and displayed hyper-reversal swimming behavior. This swimming behavior suggests high CheY-P in the cell, consistent with the *in vitro* $CheZ_{HP}$

phosphatase activity (Lertsethtakarn and Ottemann, 2010). The soft-agar migration phenotype is also consistent with the cells possessing a hyper-reversal-bias, as tumble-bias mutants perform slightly better than swim-bias mutants in this assay (Wolfe and Berg, 1989), as we observed comparing Δ*cheZ*$_{HP}$ to Δ*cheW* (Fig. 1). Several CheZ$_{HP}$ mutants that lose phosphatase activity *in vitro* (CheZ$_{HP}$ D189N, Q193R, and lacking the 12 C-terminal amino acids (Lertsethtakarn and Ottemann, 2010)) seemed to retain some *in vivo* function, as evidenced by intermediate soft-agar migration rates. One possible explanation for this phenotype is that these CheZ$_{HP}$ variants retain the weak ability to bind CheY-P. In this case, they might sequester some CheY-P away from the flagellar motor to allow slightly more normal switching between reversals and forward swimming. Similarly, Sanna and Simon (Sanna and Simon, 1996) reported that very high or very low levels of *E. coli* CheZ caused loss of soft agar migration, highlighting the idea that there is a range of CheY-P levels that supports normal soft agar movement. *H. pylori* intrinsic CheY dephosphorylation is quite fast—0.28 s^{-1}—a rate that is 8X faster than that of *E. coli* CheY (Lertsethtakarn and Ottemann, 2010). Thus in *H. pylori*, CheY may more readily dephosphorylate on its own and allow modest chemotaxis even without a phosphatase. Furthermore, there is precedence for the idea that there are multiple CheY-P binding regions in CheZ from work with *E. coli* CheZ; three regions of *E. coli* CheZ bind CheY-P—residues 67-71, 136-151, and the C-terminal 12 amino acids (Zhao *et al.*, 2002). Our finding that the strain bearing *cheZ*$_{HP}$ Q193R had a similar directional change bias as the Δ*cheZ*$_{HP}$ mutant, does not support this model however because there appears to be high CheY-P in this strain. An alternative idea is that the various CheZ$_{HP}$ variants retain the ability to interact with some components the chemotaxis signaling pathway. Indeed, there is evidence that CheZ$_{HP}$ has interactions with other parts of the chemotaxis pathway. Specifically, CheZ$_{HP}$ was discovered based on the finding that *cheZ*$_{HP}$ mutants were

able suppress loss of the CheW coupling protein (Terry *et al.*, 2006), and $CheZ_{HP}$ has phosphatase activity towards phosphoryl CheAY and CheV2 in addition to CheY (Lertsethtakarn and Ottemann, 2010). While we do not yet know the mechanism behind the ability of $cheZ_{HP}$ mutants to suppress loss of *cheW*, these results suggest there are as-yet poorly understood connections in the *H. pylori* chemotaxis pathway. One other consideration is that the soft agar assay monitors accumulation of chemotaxis ability over a period of days, whereas monitoring of the swimming behavior spans only seconds, so there are differences in strain behavior in this assay. Specifically, Lowenthal *et al*. found that *H. pylori* strains can have few reversals in the swimming assay, but gain the ability to reverse in the soft agar (Lowenthal, Simon, *et al.*, 2009).

In summary, we report that $CheZ_{HP}$ and ChePep localize to the pole to a complex that is distinct from the chemoreceptor-signaling and flagellar complexes. $CheZ_{HP}$ and ChePep promote each other's polar localization, and interact directly. Our findings raise the possibility that $CheZ_{HP}$-ChePep form a complex that localizes separately from the other motility-related complexes for a specific purpose. We noted that the polar localization of $CheZ_{HP}$-ChePep did not completely disappear in the absence of one, suggesting that there might be other proteins that participate in the $CheZ_{HP}$ and ChePep complex. We also report that $CheZ_{HP}$ may have additional functions or interactions in the chemotaxis pathway, beyond its phosphatase activity, based on the partial chemotaxis behavior of several $cheZ_{HP}$ mutants. Together, these findings suggest that while $CheZ_{HP}$ has conserved CheZ phosphatase function and mechanism, it has diverged significantly in other regards.

Acknowledgements

The authors would like to thank Tate Sessler and Dr. Nina Salama of the Fred Hutchison Cancer Research Center for providing genomic DNA for several mutant alleles; Dr. Karen Guillemin of the University of Oregon for providing several *H. pylori* mutant strains; Marla Hill for generating the G27 Δ*fliG::cat* strain; Kieran Collins and Samar Abedrabbo for immunofluorescence technical assistance; and Samar Abedrabbo for critical comments on the manuscript. The described project was supported by Grant Number AI050000 (to K.M.O.) from the National Institutes of Allergy and Infectious Disease (NIAID) at the National Institutes of Health and the University of California Cancer Research Coordinating Committee to K.M.O., and by the Morgridge Faculty Scholar Award and the Stanford Pediatric Research Fund to M.R.A. Its contents are solely the responsibility of the authors and do not necessarily represent the official views of the NIH.

Experimental Procedures

Bacterial strains and growth conditions

All *H. pylori* strains are listed in Table 2, and plasmids listed in Table 3. *H. pylori* strain G27 or its variants G27-MA and mG27 were used for all localization experiments. These strains are all highly related, were derived from the same parent, and behave the same for chemotaxis and motility. Strains SS1, SS2000, 26695, and J99 were used to confirm protein localization in some cases. *H. pylori* was grown under microaerobic condition at 37°C in an incubator with a gas mixture of 5-10% O_2, 10% CO_2, and 80-85% N_2, on Columbia horse blood agar (CHBA) with 5% difibrinated horse blood, or in brucella broth with 10% v/v heat inactivated fetal bovine serum (FBS) (BB10). Kanamycin was used at 15 µg/ml, and chloramphenicol was used at 10 µg/ml for selection of mutants.

Generation of cheZ$_{HP}$ mutants

Plasmid pKT30 containing *cheZ*$_{HP}$ and approximately 500 base pairs flanking the coding sequence (Terry *et al.*, 2006) was used as template for iPCR to remove the entire coding region of *cheZ$_{HP}$* using primers cheZup2 (5'-TGTCGTTCCTTGCCAATTGGTTTT) and cheZdn2 (5'-TTTTGAACCAAGTTGAATTACTCTC). The resulting iPCR product was ligated with an *aphA3-sacB* cassette (KS), cut from pKSF3 plasmid with SmaI and XmnI. This cassette confers kanamycin resistance and sucrose sensitivity. pKSF3 was generated from pKSFII (Copass *et al.*, 1997)by ligating XmnI linkers into the XhoI site. The Δ*cheZ*$_{HP}$*::KS* plasmid was transformed into *E. coli* DH10B (Durfee *et al.*, 2008)and verified by sequencing. The Δ*cheZ*$_{HP}$*::KS* plasmid was then transformed into *H. pylori* G27 wild type, via natural transformation, and selection for kanamycin resistance, to replace *cheZ$_{HP}$* with Δ*cheZ$_{HP}$::KS* cassette. The resulting kanamycin

resistant colonies were screened for sucrose sensitivity and verified by sequencing of a PCR product generated from the *cheZ*$_{HP}$ locus. This strain is called G27 Δ*cheZ*$_{HP}$::KS (Table 2), and was used as a parental strain for subsequent transformations to generate *cheZ*$_{HP}$ mutants.

Plasmids bearing *cheZ*$_{HP}$ deletion mutants were generated by iPCR as described above using primers that are available upon request. The resulting iPCR products were self-ligated and transformed into *E. coli* DH10B. The plasmids were verified by sequencing and used to transform G27 Δ*cheZ*$_{HP}$*::KS*. Kanamycin-sensitive, sucrose-resistant colonies were selected, screened, and verified by PCR and sequencing of *cheZ*$_{HP}$ loci.

Generation of flhF, flhG, hp0062, fliG, cheY, cheV1 cheV2, and fliF mutants

flhF, *flhG*, and *hp0062* mutant alleles marked with *cat* were obtained as G27 genomic DNA from Dr. Nina Salama (Fred Hutchison Cancer Research Center, Seattle WA). The DNA was used to transform *H. pylori* G27 wild type to chloramphenicol resistance. Colonies that were chloramphenicol resistant were selected and screened with PCR using primers that flank each locus. Similar approaches were used to move mutant alleles from other strains, and thus create G27 or G27-MA.

To create the *fliG* mutant, *fliG* was cloned from G27 genomic DNA by PCR using primers fliGlocusfor (5'-CACGCCTTTAATCAACTATA) and fliGlocusrev (5'-TAAAGCCGATTTTATAGCCA). The resulting PCR product was cloned into EcoRV-cut pBluescript creating vector pBS-FliG. pBS-FliG, was used as template in iPCR, with primers fliGcircfor-2 (5'-GGTAAGCTTGGTTGCCATTTTTA) and fliGcircrev-2 (5'-GATTCCAAACCGGTGAAGAGGA) that deleted most of the gene. This PCR product was gel purified and ligated with a terminator-less *cat* gene obtained from the vector pCat-mut (Terry *et*

al., 2005) using HincII, to create the vector pBS-FliG::cat-mut. pBS-FliG::cat-mut was used to transform G27 to chloramphenicol resistance.

The *cheY* allele used here was generated by digesting pKO126 with Bpu1102I, which cuts about ¼ of the way into the open reading frame, followed by creating blunt ends. This product was ligated with the *aphA-sacB* genes derived from pKSFII cut with SmaI and XhoI, followed by blunt end generation, to create pKO126i. pKO126i was used to transform G27 to kanamycin resistance.

The double mutant in *cheV1* and *cheV2* was constructed using the allelic replacement strategy as previously described (Chalker *et al.*, 2001). First, G27-MA was naturally transformed with a construct replacing *cheV1* with a kanamycin resistance cassette (aphA3) using the primers CheV1-1 (5'-CTAGCGAGTTTAGGAAGCAATTG), CheV1-2 (5'-ATGGTTCGCTGGGTTTATCACTATCAGCCATGATTTCCCCTT), CheV1-3 (5'-TTACTAGGATGAATTGTTTTAGTACCCAATGGTAAAACCTTATTGGAGC), and CheV1-4 (5'-GCTCGCACAACACCCGTTCAATC). Mutants were screened for kanamycin resistance and confirmed by PCR. Then G27-MA Δ*cheV1*::aphA3 mutants were naturally transformed with a construct replacing *cheV2* with an erythromycin resistance cassette using the following primers, CheV2-1 (5'-AGCGTTAGTAACAAGCTCTCC), CheV2-2 (5'-TACTGCAATCTGATGCGATTATTGCTAATTTCCCCTAAAGCCCTATC), CheV2-3 (5'-TTCAATAGCTATAAATTATTTAATAAGTAAGAATCGCTACTCATGGACGAATTG) and CheV2-4 (5'-GGTATTTCAAGCGCAAATCTTCATTC). Transformants were screened for both kanamycin and erythromycin resistance and confirmed by sequencing.

Mutants in *fliF* were generated by replacing *fliF* with a *cat* cassette followed by selection of transformants on chloramphenicol. The allelic replacement construct was generated by join-

ing the *cat* cassette with sequence upstream of *fliF* with primers fliF-1(5'-TCGCAGAAACTTAGCGCTTGG), fliF-2(5'-ATCCACTTTTCAATCTATATCAAGCAAAGCGGTGATTAAAACC) and downstream fliF-3(5'-CCCAGTTTGTCGCACTGATAAAAGATAAAAGGTTAAAAATGGCAACC), fliF-4(5'-TGGAGATCTCAGCTTTCATTTCA). The resulting G27-MA Δ*fliF* mutants were confirmed by sequence analysis.

Generation of mutant lacking all chemoreceptors

Construction of the Δ*tlpA*, Δ*tlpB*, Δ*tlpC* and Δ*tlpD* individual mutants has been described (Rader *et al.*, 2011). In all cases, the resulting mutations were verified using PCR and sequencing for clean deletions. To create multiple receptor mutants, we started with mG27 Δ*tlpA* (KO1002) and transformed with genomic DNA bearing Δ*tlpD::cat* from KO1006, to create Δ*tlpA* Δ*tlpD* (KO1009). After verification, this strain was transformed with genomic DNA with *tlpB*::kan-sac, followed by transformation to sucrose resistance/kanamycin sensitivity using KO1004 (Δ*tlpB*) chromosome. This created strain KO1015 which was then transformed with KO1005 chromosome (Δ*tlpC::kan*) to create Δ*tlpA* Δ*tlpB* Δ*tlpC::kan* Δ*tlpD::cat* (KO1021).

Creation and pre-absorption of antibodies

Antibodies that recognize ChePep, CheY, and all *H. pylori* chemoreceptors, called TlpA22, have been described previously (Williams *et al.*, 2007; Lowenthal, Hill, *et al.*, 2009; Howitt *et al.*, 2011). Antibodies that recognize CheAY, CheV1, or $CheZ_{HP}$ were generated in rabbits using either purified His-CheAY, CheV1, or $CheZ_{HP}$ (Lertsethtakarn and Ottemann, 2010). For pre-absorption of these antibodies, strain *H. pylori* G27 Δ$cheZ_{HP}$*::KS*, Δ$cheZ_{HP}$, Δ*cheAY::cat,* Δ*cheV1::cat,* Δ*tlp's, or* Δ*chepep* were used. For the preabsorption, each *H. pylori*

strain was grown overnight on three CHBA plates. Cells were resuspended in 2ml 1X PBS (10X: 80g NaCl, 2g KCl,11.5g $Na_2HPO4 \cdot 7H_2O$, 2g KH_2 PO_4 to 1L adjusted to pH 7.3) collected by centrifugation and resuspended in 1ml PLP (75mM $NaPO_4$, pH 7.4, 2.5mM NaCl, 2% para-formaldehyde in 1X PBS) followed by 10 minutes room temperature incubation to fix the cells. Cells were collected by centrifugation, and washed with 1XPBS three times. To permeabilize the cells, 1ml of permeabilizing buffer (3% BSA, 1% saponin, 0.1% triton X-100, 0.02% sodium azide in PBS) was added and cells were incubated at room temperature for 10 minutes. Permeabilized cells were centrifuged as above to remove supernatant. Cells were resuspended in 700µl of permeabilizing buffer and respective antibody was added at a 1:100 dilution. The mixture was incubated with rotation overnight at 4^oC. Cells were removed by centrifugation and the supernatant was collected. To check for complete absorption of the antibody, western analysis was performed.

Immunofluorescence

For immunofluorescence analysis, liquid cultures of the *H. pylori* strains to be analyzed were grown in BB10 for 6 hours (exponential phase). The culture was visually inspected for motility before slide preparation. 40-65 µl of the culture was placed on a poly-L-lysine coated slides (Ted Pella, Inc), followed by addition of PLP and incubation at room temperature for 10 minutes. These fixed cells were then permeabilized with permeabilizing buffer at room temperature for 10 minutes. Pre-absorbed primary anti-$CheZ_{HP}$, -His-CheAY, -CheV1, or -ChePep were each used at 1:200, anti-TlpA22 was used at 1:1000, and chicken anti-*H. pylori* (AgriSera AB) was used at 1:500 dilution. The reactions were incubated at room temperature for 30 minutes and the cells were washed with blocking buffer (3% BSA, 0.1% TritonX-100 in 1X PBS) 3 times. Goat anti-rabbit conjugated with Alexa Fluor® 594 (Invitrogen) and goat anti-chicken conjugated with

Alexa Fluor® 488 (Invitrogen) were added at 1:300 and 1:500 dilutions, respectively, and incubated in the dark at room temperature for 30 minutes. The samples were washed as above. A drop of Vectashield® with DAPI (Vector Laboratories, Inc.) was added and the samples were sealed with coverslips.

Immunofluorescent cells were viewed using a Nikon ECLIPSE E600 microscope and SPOT software Version 4.7 (Diagnostic instruments, inc.), using a Plan Flour 100X (Nikon) objective. A Texas Red® (Chroma) filter cube was used to view and capture emission from Alexa Fluor® 594 (red) and FITC/GFP (Chroma) filter cube was used to view and capture emission from Alexa Fluor® 488 (green). Images were taken in color for each fluor separately and merged in Adobe® Photoshop® CS2 version 9.0.2 (Adobe®).

Immunoprecipitation, cell fractionation, and immunoblotting

For immunoprecipitation, $CheZ_{HP}$ and ChePep were purified as a GST-fusion proteins, as described previously (Lertsethtakarn and Ottemann, 2010; Howitt *et al.*, 2011). For co-immunoprecipitation experiments, the GST-tag was removed using Prescission Protease (GE Healthcare Life Sciences). Anti-$CheZ_{HP}$ or anti-ChePep antibodies were conjugated to beads, using Protein A-coupled magnetic Dynabeads (Life Technologies) and crosslinking with BS^3. Equimolar ChePep and $CheZ_{HP}$ (9 μM each) were mixed, allowed to form complexes for 30-60 minutes at room temperature, diluted to 3μM, and then incubated with the antibody-bound beads as directed by the manufacturers' protocols. Beads were washed four-times with phosphate buffered saline plus 0.04% Tween-20, before elution with pH 2.8 glycine, following the manufacturers protocols.

To test for expression and differential solubility of $CheZ_{HP}$ and ChePep in the different mutant backgrounds, *H. pylori* cells grown for < 24 hours in microaerobic conditions were harvested directly from blood agar plates into 0.5% Tween-20, 50mM Tris pH 7.4, 200 mM NaCl, 1 mM EDTA, 1M PMSF, vortexed and incubated for 15 minutes on ice. The lysates were then centrifuged at 15,000Xg and the soluble fraction diluted 1:1 in 2X SDS sample buffer. The Tween-insoluble pellets were resuspended in equal volumes of SDS sample buffer, prior to boiling, separation by SDS-PAGE and immunoblotting as described above.

For immunoblots, samples were electrophoreses on either 8-16% or 10% SDS-PAGE gels. After transfer to polyvinylidene difluoride (PVDF) membranes, proteins were detected using either rabbit anti-$CheZ_{HP}$, rabbit anti-ChePep, or rabbit anti-CheY. Fluorescent secondary antibodies were used for the solubility experiments with anti-$CheZ_{HP}$ followed by goat anti-rabbit Alexa Fluor 660, anti-ChePep followed by goat anti-rabbit Alex Fluor 800, anti-CheY with both goat anti-rabbit Alex Fluor 660 and 800. All membranes were scanned with a Licor-Odyssey scanner and overlayed to create a single western blot. HRP-conjugated goat-anti rabbit antibodies (Thermo-Fisher) were used for the co-immunoprecipitation experiments.

Soft agar migration assay

$cheZ_{HP}$ mutants were inoculated in BB10 containing 0.35% (w/v) of agar (Bacto). Each plate was also inoculated with *H. pylori* wild type and non-chemotactic Δ*cheW* to serve as controls. Cultures were incubated as described above for 4-5 days. The diameter of the bacterial colony was measured at the end of incubation period.

Analysis of swimming behavior

H. pylori strains were cultured for six hours with shaking or overnight without shaking in BB10. The swimming behavior of each culture was viewed and recorded using Simple PCI version 5.3.1. (Compix Inc., Imaging Systems) and Hamamatsu Digital Camera C4742-98 on a Nikon ECLIPSE E600 microscope at 100X magnification. At least twenty films were recorded for each culture, from at least two independent biological replicates. Files were randomized to conceal the identity of analyzed strain. For each *H. pylori* strain, at least 150 cells were tracked for clear directional changes for 5 seconds, using hand-tracing of each swimming bacteria.

Statistical analysis

Two sample Student's *t*-test in SYSTAT 13 © (Systat Software, Inc.) was used to perform statistical analyses.

Figure Legends.

Figure 1. (A) Schematic of $CheZ_{HP}$ protein. The active site region is indicated by a horizontal line above. The N terminal region (1-39) contains six copies of a highly charged amino acid sequence (KEE). The active site residues are indicated by vertical lines (D189 and Q193R). The C terminal region (241-253) binds CheY-P. The portions retained in the original Δ*cheZ*$_{HP}$::cat allele are shown with thick horizontal lines below the $CheZ_{HP}$ schematic. **(B)** Soft agar migration rates of *H. pylori* G27 wild type (WT), Δ*cheW*, and *cheZ*$_{HP}$ isogenic mutants. Strains were stabbed into Brucella broth-FBS soft agar, and the diameter of the expanded colony measured after 4-5 days. The data represents the average of at least two biological replicates with at least three technical replicates. Error bars show standard error. * indicates significantly different from WT (P value <0.05) using Student's *t* test.

Figure 2. Swimming behavior of *cheZ*$_{HP}$ mutant strains. *H. pylori* G27 cells in Brucella Broth with FBS (BB10) were filmed using microscopy, and then the number of directional changes in five seconds were counted. The number of examined cells (*n*) and average directional changes per cell (indicated by black solid lines) are as follow: WT (*n* = 230, 1.8), Δ*cheZ*$_{HP}$ (*n* =156, 4.0), and *cheZ*$_{HP}$ Q193R (n = 155, 4.6), *cheZ*$_{HP}$ N-only (n=186, 7.4), Δ*cheZ*$_{HP}$*::cat* (n=211, 0.03). At least two biological replicates were used for each strain. ** indicates significantly different from wild type (P value <0.01) using Student's *t* test.

Figure 3. *H. pylori* chemoreceptors and core chemotaxis signaling proteins form a polar cluster anchored by the chemoreceptors. The protein examined is indicated across the top, and the strain

backgrounds are indicated in white writing within each panel. CheAY, CheV1, and the chemoreceptors are shown in red, detected by immunofluorescence using rabbit polyclonal anti-CheAY, anti-CheV1, or anti-TlpA22 respectively, followed by incubation with anti-rabbit antibodies conjugated with Alexa Fluor® 594 to fluoresce red. *H. pylori* cells are green, visualized by chicken anti-*H. pylori* antibodies, followed by anti-chicken antibodies conjugated with Alexa Fluor® 488, to fluoresce green. Multiple bacteria are shown; in some cases these were captured from independent images.

Figure 4. $CheZ_{HP}$ and ChePep form a polar cluster that is independent from chemotaxis and flagellar-related proteins. Protein analyzed indicated above each set of relevant panels in a color matching the detection color. Strain background indicated in white writing within each panel. Multiple bacteria are shown for each mutant; in some cases these were captured from independent images. Scale bar represents 1 μm. **A**. $CheZ_{HP}$ (red) was detected using anti-$CheZ_{HP}$ antibodies, followed by secondary antibodies conjugated to Alexa Fluor® 594 to fluoresce red. *H. pylori* cells (green) were visualized chicken anti-*H. pylori* antibodies, followed by secondary conjugated with Alexa Fluor® 488. **B**. $CheZ_{HP}$ and ChePep localization in chemotaxis signaling mutants. $CheZ_{HP}$ (red) was visualized as in Panel A. ChePep (green) was visualized using anti-ChePep antibodies, followed by secondary anti-rabbit antibodies conjugated to Alexa Fluor 488, while whole bacteria were visualized using chicken anti-*H. pylori* followed by secondary antibodies conjugated to Alexa Fluor 594 to fluoresce red. **C.** $CheZ_{HP}$ and ChePep localization in flagellar mutants. $CheZ_{HP}$ and ChePep visualized as in Panel A and B, respectively. **D.** $CheZ_{HP}$ and ChePep are mutually dependent on each other. $CheZ_{HP}$ and ChePep visualized as in Panel A and B, respectively, with the addition of cells being visualized by DAPI DNA staining (blue).

Figure 5. ChePep and $CheZ_{HP}$ are expressed independently of each other. Western blot analysis of 8-16% gradient gels of ChePep, $CheZ_{HP}$ and CheY association with triton-insoluble (Pellet, P) and soluble fractions (S). The bottom panel shows coomassie stained identical samples. Molecular weight in kilodaltons indicated at the left of each panel. The predicted molecular weight of ChePep is 56 kilodaltons, but it migrates slower in SDS-PAGE presumably due to its high charge.

Figure 6. $CheZ_{HP}$ N and C termini are dispensable for polar localization of $CheZ_{HP}$ (left panels, red) and ChePep (right panels, green). $CheZ_{HP}$ and ChePep were detected by immunofluorescence as described in Fig. 4. Protein analyzed indicated in each set of relevant panels in a color matching the detection color. Strain background indicated in white writing within each panel. Multiple bacteria are shown; in some cases these were captured from independent images.

Figure 7. $CheZ_{HP}$ and ChePep interact directly. **A.** Coomassie-stained SDS-PAGE gel of purified ChePep (left) and $CheZ_{HP}$ (right) proteins. Molecular weight in kilodaltons indicated at the left of each panel. **B.** Co-immunoprecipitation of $CheZ_{HP}$ and ChePep, analyzed by western blotting of 10% SDS-PAGE gels with anti-$CheZ_{HP}$. From left to right: (1) Pep: the ChePep starting material (2) $CheZ_{HP}$: the $CheZ_{HP}$ starting materials; (3-5) Immunoprecipitation (IP) with anti-$CheZ_{HP,}$ incubated with a mixture of ChePep+$CheZ_{HP}$ (both), ChePep (P) or $CheZ_{HP}$ (Z); (6-8) IP with anti-ChePep, incubated with each set of proteins as in (3-5). The positions of ChePep and $CheZ_{HP}$ are indicated on the right.

658 **Table 1. $CheZ_{HP}$ and ChePep cellular localization in different mutant backgrounds.**

***H. pylori* strain**	**$CheZ_{HP}$**		**ChePep**	
	Location (N)	**Strains**	**Location (N)**	**Strains**
WT	Pole (176)	G27, mG27, G27-MA, SS1	Pole (187)	G27, G27-MA, SS1, SS2000, 26695, J99
tlpABCD (Δ*tlp's*)	Pole (82)	mG27	Pole (117)	mG27
cheAY	Pole (81)	G27, G27-MA, SS1	Pole (90)	G27-MA, SS1
cheW	Pole (43)	G27, G27-MA, SS1	Pole (44)	G27-MA, SS1
cheV1	Pole (38)	G27, G27-MA, SS1	Pole (30)	G27-MA, SS1
cheV2	Pole (60)	G27, G27-MA, SS1	Pole (54)	G27-MA, SS1
cheV1 cheV2	Pole	G27-MA	Pole	G27-MA
cheV3	Pole (75)	G27, G27-MA, SS1	Pole (63)	G27-MA
cheY	Pole (11)	G27, G27-MA, SS1	Pole (79)	G27-MA, SS1
Δ$cheZ_{HP}$ or Δ$cheZ_{HP::KS}$	Not detected (76)	G27, G27-MA, SS1	Diffuse (38)	G27-MA

fliG	Pole (72)	G27		
fliM	Pole (81)	G27	Pole (27)	G27-MA
fliN	Pole (69)	G27		
fliY	Pole (72)	G27		
fliF	Pole (58)	G27-MA	Pole (23)	G27-MA
motB	Pole (75)	G27	Pole (54)	G27-MA
flhA	Pole (76)	G27	Pole (76)	G27
flhF	Pole (33)	G27	Pole (150)	G27
fliA	Pole (77)	G27		
flhG	Pole (33)	G27		
hp0062	Pole (19)	G27		
chePep	Diffuse (27)	G27-MA, G27, SS1, PMSS1	Not detected	G27-MA, G27, SS1, PMSS1
$cheZ_{HP}$ ΔN_{39}	Pole (138)	G27		
$cheZ_{HP}$ N-only	ND (70)	G27		
$cheZ_{HP}$ ΔC_{12}	Pole (20)	G27	Pole (150)	G27
$cheZ_{HP}$ C-only	ND (16)	G27		

659

N indicates number of individual cells viewed, from > 1 biological replicate; in all cases, CheZHP was observed as indicated. When more than one strain is listed, localization enumeration was done in the first strain and verified in the others..

663 **Table 2: *H. pylori* strains used in this study**

***H. pylori* strains**	**Strain #**	**Genotype/Description**	**Reference/source**
G27		Wild type	(Censini *et al.*, 1996)/From Nina Salama
mG27	KO625	G27, mouse-adapted	(Castillo *et al.*, 2008)
G27-MA		G27, MDCK cells adapted	(Amieva *et al.*, 2003)
SS1		Wild type, mouse adapted	(Lee *et al.*, 1997)
SS2000		Wild type	(Thompson *et al.*, 2004)
PMSS1		Wild type, Parent of strain SS1, not mouse adapted	(Arnold *et al.*, 2011)
26695		Wild type	(Tomb *et al.*, 1997)
J99		Wild type	(Alm *et al.*, 1999)
G27 Δ$cheZ_{HP}$::*KS*	KO1269	G27 Δ$cheZ_{HP}$::*aphA3/sacB*	This study
G27 Δ$cheZ_{HP}$	KO1315	KO1269 Δ$cheZ_{HP}$ (entire coding region deleted)	This study
G27 Δ$cheZ_{HP}$::$cheZ_{HP}$	KO1304	KO1269 Δ$cheZ_{HP}$:: $cheZ_{HP}$ (complement)	This study
G27 Δ$cheZ_{HP}$::*cat*	KO1325	G27 ΔΔ$cheZ_{HP}$::*cat* (retains coding potential for the first 13 and last 12 amino acids)	This study; allele originally published in (Terry *et al.*, 2006)
G27 $cheZ_{HP}$ Q193R	KO1307	KO1269 Δ$cheZ_{HP}$::$cheZ_{HP}$ Q193R	This study
G27 $cheZ_{HP}$ D189N	KO1306	KO1269 Δ$cheZ_{HP}$::$cheZ_{HP}$ D189N	This study
G27 $cheZ_{HP}$ ΔN_{39}	KO1313	KO1269 Δ$cheZ_{HP}$:: $cheZ_{HP}$ ΔN (deletion of amino acids 1-39)	This study
G27 $cheZ_{HP}$ N-only	KO1273	KO1269 Δ$cheZ_{HP}$:: $cheZ_{HP}$ 1-39 (retains amino acids 1-39)	This study
G27 $cheZ_{HP}$ ΔC_{12}	KO1300	KO1269 Δ$cheZ_{HP}$:: $cheZ_{HP}$ ΔC (deletion of C-terminal 12 amino acids)	This study
G27 $cheZ_{HP}$ C-only	KO1312	KO1269 Δ$cheZ_{HP}$:: $cheZ_{HP}$ C-only (retains amino acids 241-253)	This study
G27 Δ*cheW*	KO851	G27 Δ*cheW::aphA3*	(Terry *et al.*, 2005)
G27 Δ*cheAY*	KO857	G27 Δ*cheAY::cat (also called* Δ*cheA::cat)*	This study; *cheAY* allele published in (Terry *et al.*, 2005)

G27 Δ*cheY*	KO1250	G27 Δ*cheY::aphA3-sacB*	This study
G27 Δ*cheV1*	KO1277	G27 Δ*cheV1::cat*	This study; *cheV1* allele published in (Low-enthal, Simon, *et al.*, 2009)
G27 Δ*cheV2*	KO1278	G27 Δ*cheV2::cat*	This study; *cheV2* allele published in (Low-enthal, Simon, *et al.*, 2009)
G27 Δ*cheV3*	KO1279	G27 Δ*cheV3::cat*	This study; *cheV3* allele published in (Low-enthal, Simon, *et al.*, 2009)
mG27 Δ*tlpA*	KO1002	mG27 Δ*tlpA*	(Rader *et al.*, 2011)
mG27 Δ*tlpB*	KO1004	mG27 Δ*tlpB*	(Rader *et al.*, 2011)
mG27 Δ*tlpC*	KO1005	mG27 Δ*tlpC*::*aphA3*	(Rader *et al.*, 2011)
mG27 Δ*tlpD*	KO1006	mG27 Δ*tlpD*::*cat*	(Rader *et al.*, 2011)
mG27 Δ*tlpB::kan-sac*	KO1003	mG27 Δ*tlpB*::*aphA3-sacB*	(Rader *et al.*, 2011)
mG27 Δ*tlpA* Δ*tlpD*	KO1009	KO1002 Δ*tlpD*::*cat*	This study
mG27 Δ*tlpA* Δ*tlpB* Δ*tlpD*	KO1015	KO1009 Δ*tlpB*	This study
mG27 Δ*tlpA* Δ*tlpB* Δ*tlpC* Δ*tlpD* (Δ*tlps*)	KO1021	KO1015 Δ*tlpC::aphA3*	This study
G27-MA Δ*chePep*		G27-MA Δ*chePep::cat*	(Howitt *et al.*, 2011)
G27-MA ChePep*		G27-MA Δ*chePep::cat rdxA::chePep-ahpA3*	(Howitt *et al.*, 2011)
G27-MA Δ*cheV1* Δ*cheV2*			This study
H. pylori G27 *flhA*	KO1284	G27 *flhA::kan*	(Rader *et al.*, 2007). Gift of Karen Guillemin.

H. pylori G27 Δ*flhF*	KO1367	G27 Δ*flhF::cat* (165 bp deletion)	This study. Allele provided by Nina Salama (Fred Hutchison Cancer Research Center, Seattle WA).
H. pylori G27 Δ*flhG*	KO1328	G27 Δ*flhG::cat* (62 bp deletion)	This study. Allele provided by Nina Salama (Fred Hutchison Cancer Research Center, Seattle WA).
H. pylori G27 *fliA*	KO1285	G27 *fliA::kan*	(Rader *et al.*, 2007). Gift of Karen Guillemin.
G27-MA Δ*fliF*		G27Δ*fliF::cat*	This study
G27 Δ*fliG*	KO1063	G27 *ΔfliG::cat*	This study
G27 Δ*fliM*	KO1060	G27 *ΔfliM::cat*	(Lowenthal, Hill, *et al.*, 2009)
G27 *fliN* (KO1061)	KO1061	G27 *ΔfliN::cat*	(Lowenthal, Hill, *et al.*, 2009)
G27 *fliY* (KO1062)	KO1062	G27 *ΔfliY::cat*	(Lowenthal, Hill, *et al.*, 2009)
G27 *motB*	KO489	G27 *motB::aphA3-sacB*	(Ottemann and Lowenthal, 2002)
G27 Δ*hp0062*	KO1310	*G27_57/hp0062::cat*	This study. Allele provided by Nina Salama (Fred Hutchison Cancer Research Center, Seattle WA).

Table 3. Plasmids used in this study

Plasmid	Characteristic	Reference
pKT30	pBluescript::*hp0170*$_{SS1}$ (*cheZ*$_{HP}$)	**(Terry *et al.*, 2006)**
pKO126	pBluescript::*cheY*$_{SS1}$	**(Terry *et al.*, 2005)**
pKSFII	pBluescript::*aphA3-sacB* (kan-sac or KS)	**(Copass *et al.*, 1997)**
pKSF3	pKSFII XhoI::XmnI	This study
pBS-FliG	pBluescript::*fliG*$_{G27}$	This study
pBS-FliG::cat-mut	pBluescript::*fliG*$_{G27}$*::cat-mut*	This study
pKO126i	pKO126::*aphA3-sacB*	This study
pCat-mut	pBluescript::*cat-mut* (lacking tran-scriptional terminator)	**(Terry *et al.*, 2005)**

Literature cited

Alexander, R.P., Lowenthal, A.C., Harshey, R.M., and Ottemann, K.M. (2010) CheV: CheW-like coupling proteins at the core of the chemotaxis signaling network. *Trends Microbiol* **18**: 494–503.

Allan, E., Dorrell, N., Foynes, S., Anyim, M., and Wren, B.W. (2000) Mutational analysis of genes encoding the early flagellar components of *Helicobacter pylori:* evidence for transcriptional regulation of flagellin A biosynthesis. *J Bacteriol* **182**: 5274–5277.

Alm, R.A., Ling, L.S., Moir, D.T., King, B.L., Brown, E.D., Doig, P.C., *et al.* (1999) Genomic-sequence comparison of two unrelated isolates of the human gastric pathogen *Helicobacter pylori. Nature* **397**: 176–180.

Amieva, M.R., Vogelmann, R., Covacci, A., Tompkins, L.S., Nelson, W.J., and Falkow, S. (2003) Disruption of the epithelial apical-junctional complex by *Helicobacter pylori* CagA. *Science* **300**: 1430–1434.

Arnold, I.C., Lee, J.Y., Amieva, M.R., Roers, A., Flavell, R.A., Sparwasser, T., and Müller, A. (2011) Tolerance rather than immunity protects from *Helicobacter pylori*-induced gastric preneoplasia. *Gastroenterology* **140**: 199–209.

Blat, Y., and Eisenbach, M. (1996) Conserved C-terminus of the phosphatase CheZ is a binding domain for the chemotactic response regulator CheY. *Biochemistry* **35**: 5679–5683.

Briegel, A., Ortega, D.R., Tocheva, E.I., Wuichet, K., Li, Z., Chen, S., *et al.* (2009) Universal architecture of bacterial chemoreceptor arrays. *Proc Natl Acad Sci USA* **106**: 17181–17186.

Cantwell, B.J., and Manson, M.D. (2009) Protein domains and residues involved in the CheZ/CheAS interaction. *J Bacteriol* **191**: 5838–5841.

Cantwell, B.J., Draheim, R.R., Weart, R.B., Nguyen, C., Stewart, R.C., and Manson, M.D. (2003) CheZ phosphatase localizes to chemoreceptor patches via CheA-short. *J Bacteriol* **185**: 2354–2361.

Castillo, A.R., Woodruff, A.J., Connolly, L.E., Sause, W.E., and Ottemann, K.M. (2008) Recombination-Based In Vivo Expression Technology Identifies *Helicobacter pylori* Genes Important for Host Colonization. *Infect Immun* **76**: 5632–5644.

Censini, S., Lange, C., Xiang, Z., Crabtree, J.E., Ghiara, P., Borodovsky, M., *et al.* (1996) *cag*, a pathogenicity island of *Helicobacter pylori*, encodes type I-specific and disease-associated virulence factors. *Proc Natl Acad Sci USA* **93**: 14648–14653.

Cerda, O., Rivas, A., and Toledo, H. (2003) *Helicobacter pylori s*train ATCC700392 encodes a methyl-accepting chemotaxis receptor protein (MCP) for arginine and sodium bicarbonate. *FEMS Microbiol Lett* **224**: 175–181.

Chalker, A.F., Minehart, H.W., Hughes, N.J., Koretke, K.K., Lonetto, M.A., Brinkman, K.K., *et al.* (2001) Systematic identification of selective essential genes in *Helicobacter pylori* by genome prioritization and allelic replacement mutagenesis. *J Bacteriol* **183**: 1259–1268.

Copass, M., Grandi, G., and Rappuoli, R. (1997) Introduction of unmarked mutations in the *Helicobacter pylori vacA* gene with a sucrose sensitivity marker. *Infect Immun* **65**: 1949–1952.

Croxen, M.A., Sisson, G., Melano, R., and Hoffman, P.S. (2006) The *Helicobacter pylori* chemotaxis receptor TlpB (HP0103) is required for pH taxis and for colonization of the gastric mucosa. *J Bacteriol* **188**: 2656–2665.

Durfee, T., Nelson, R., Baldwin, S., Plunkett, G., Burland, V., Mau, B., *et al.* (2008) The complete genome sequence of *Escherichia coli* DH10B: insights into the biology of a laboratory workhorse. *J Bacteriol* **190**: 2597–2606.

Foynes, S., Dorrell, N., Ward, S.J., Stabler, R.A., McColm, A.A., Rycroft, A.N., and Wren, B.W. (2000) *Helicobacter pylori* possesses two CheY response regulators and a histidine kinase sensor, CheA, which are essential for chemotaxis and colonization of the gastric mucosa. *Infect Immun* **68**: 2016–2023.

Greenfield, D., McEvoy, A.L., Shroff, H., Crooks, G.E., Wingreen, N.S., Betzig, E., and Liphardt, J. (2009) Self-Organization of the *Escherichia coli* Chemotaxis Network Imaged with Super-Resolution Light Microscopy. *PLoS Biol* **7**: e1000137.

Hess, J.F., Oosawa, K., Kaplan, N., and Simon, M.I. (1988) Phosphorylation of three proteins in the signaling pathway of bacterial chemotaxis. *Cell* **53**: 79–87.

Howitt, M.R., Lee, J.Y., Lertsethtakarn, P., Vogelmann, R., Joubert, L.-M., Ottemann, K.M., and Amieva, M.R. (2011) ChePep controls *Helicobacter pylori* Infection of the gastric glands and chemotaxis in the *Epsilonproteobacteria*. *mBio* **2**: e00098–11.

Jiménez-Pearson, M.-A., Delany, I., Scarlato, V., and Beier, D. (2005) Phosphate flow in the chemotactic response system of *Helicobacter pylori*. *Microbiology (Reading, Engl)* **151**: 3299–3311.

Josenhans, C., and Suerbaum, S. (2002) The role of motility as a virulence factor in bacteria. *Int J Med Microbiol* **291**: 605–614.

Kazmierczak, B.I., and Hendrixson, D.R. (2013) Spatial and numerical regulation of flagellar biosynthesis in polarly flagellated bacteria. *Mol Microbiol* **88**: 655–663.

Kentner, D., and Sourjik, V. (2009) Dynamic map of protein interactions in the Escherichia coli chemotaxis pathway. **5**: 238.

Lee, A., O'Rourke, J., De Ungria, M.C., Robertson, B., Daskalopoulos, G., and Dixon, M.F. (1997) A standardized mouse model of *Helicobacter pylori* infection: introducing the Sydney strain. *Gastroenterology* **112**: 1386–1397.

Lertsethtakarn, P., and Ottemann, K.M. (2010) A remote CheZ orthologue retains phosphatase function. *Mol Microbiol* **77**: 225–235.

Lertsethtakarn, P., Ottemann, K.M., and Hendrixson, D.R. (2011) Motility and Chemotaxis in *Campylobacter* and *Helicobacter*. *Annu Rev Microbiol* **65**: 389–410.

Lipkow, K. (2006) Changing cellular location of CheZ predicted by molecular simulations. *PLoS Comput Biol* **2**: e39.

Lowenthal, A.C., Hill, M., Sycuro, L.K., Mehmood, K., Salama, N.R., and Ottemann, K.M. (2009) Functional analysis of the *Helicobacter pylori* flagellar switch proteins. *J Bacteriol* **191**: 7147–7156.

Lowenthal, A.C., Simon, C., Fair, A.S., Mehmood, K., Terry, K., Anastasia, S., and Ottemann, K.M. (2009) A fixed-time diffusion analysis method determines that the three *cheV* genes of *Helicobacter pylori* differentially affect motility. *Microbiology* **155**: 1181–1191.

Maddock, J.R., and Shapiro, L. (1993) Polar location of the chemoreceptor complex in the *Escherichia coli* cell. *Science* **259**: 1717–1723.

Miller, L.D., Russell, M.H., and Alexandre, G. (2009) Diversity in bacterial chemotactic responses and niche adaptation. *Adv Appl Microbiol* **66**: 53–75.

Niehus, E., Gressmann, H., Ye, F., Schlapbach, R., Dehio, M., Dehio, C., *et al.* (2004) Genome-wide analysis of transcriptional hierarchy and feedback regulation in the flagellar system of *Helicobacter pylori*. *Mol Microbiol* **52**: 947–961.

Ottemann, K.M., and Lowenthal, A.C. (2002) *Helicobacter pylor*i uses motility for initial colonization and to attain robust infection. *Infect Immun* **70**: 1984–1990.

Ping, L., Weiner, B., and Kleckner, N. (2008) Tsr-GFP accumulates linearly with time at cell poles, and can be used to differentiate 'old' versus “new” poles, in Escherichia coli. *Mol Microbiol* **69**: 1427–1438.

Pittman, M.S., Goodwin, M., and Kelly, D.J. (2001) Chemotaxis in the human gastric pathogen *Helicobacter pylori*: different roles for CheW and the three CheV paralogues, and evidence for CheV2 phosphorylation. *Microbiology (Reading, Engl)* **147**: 2493–2504.

Polk, D.B., and Peek, R.M. (2010) Helicobacter pylori: gastric cancer and beyond. *Nat Rev Cancer* **10**: 403–414.

Rader, B.A., Campagna, S.R., Semmelhack, M.F., Bassler, B.L., and Guillemin, K. (2007) The Quorum-Sensing Molecule Autoinducer 2 Regulates Motility and Flagellar Morphogenesis in *Helicobacter pylori*. *J Bacteriol* **189**: 6109–6117.

Rader, B.A., Wreden, C., Hicks, K.G., Sweeney, E.G., Ottemann, K.M., and Guillemin, K. (2011) *Helicobacter pylori* perceives the quorum-sensing molecule AI-2 as a chemorepellent via the chemoreceptor TlpB. *Microbiology* **157**: 2445–2455.

Rain, J.C., Selig, L., De Reuse, H., Battaglia, V., Reverdy, C., Simon, S., *et al.* (2001) The protein-protein interaction map of *Helicobacter pylori*. *Nature* **409**: 211–215.

Rao, C.V., Kirby, J.R., and Arkin, A.P. (2005) Phosphatase localization in bacterial chemotaxis: divergent mechanisms, convergent principles. *Phys Biol* **2**: 148–158.

Salama, N.R., Hartung, M.L., and Müller, A. (2013) Life in the human stomach: persistence strategies of the bacterial pathogen *Helicobacter pylori*. *Nat Rev Microbiol*.

Sanna, M.G., and Simon, M.I. (1996) In vivo and in vitro characterization of *Escherichia coli* protein CheZ gain- and loss-of-function mutants. *J Bacteriol* **178**: 6275–6280.

Schweinitzer, T., Mizote, T., Ishikawa, N., Dudnik, A., Inatsu, S., Schreiber, S., *et al.* (2008) Functional characterization and mutagenesis of the proposed behavioral sensor TlpD of *Helicobacter pylori*. *J Bacteriol* **190**: 3244–3255.

Silversmith, R.E. (2010) Auxiliary phosphatases in two-component signal transduction. *Curr Opin Microbiol* **13**: 177–183.

Sourjik, V., and Armitage, J.P. (2010) Spatial organization in bacterial chemotaxis. *EMBO J* **29**: 2724–2733.

Sweeney, E.G., Henderson, J.N., Goers, J., Wreden, C., Hicks, K.G., Foster, J.K., *et al.* (2012) Structure and proposed mechanism for the pH-sensing *Helicobacter pylori* chemoreceptor TlpB. *Structure* **20**: 1177–1188.

Szurmant, H., Bunn, M.W., Cannistraro, V.J., and Ordal, G.W. (2003) *Bacillus subtilis* hydrolyzes CheY-P at the location of its action, the flagellar switch. *J Biol Chem* **278**: 48611–48616.

Terry, K., Go, A.C., and Ottemann, K.M. (2006) Proteomic mapping of a suppressor of non-chemotactic *cheW* mutants reveals that *Helicobacter pylori* contains a new chemotaxis protein. *Mol Microbiol* **61**: 871–882.

Terry, K., Williams, S.M., Connolly, L.L., and Ottemann, K.M. (2005) Chemotaxis plays multiple roles during *Helicobacter pylori* animal infection. *Infect Immun* **73**: 803–811.

Thompson, L.J., Danon, S.J., Wilson, J.E., O'Rourke, J.L., Salama, N.R., Falkow, S., *et al.* (2004) Chronic *Helicobacter pylori* infection with Sydney strain 1 and a newly identified mouse-adapted strain (Sydney strain 2000) in C57BL/6 and BALB/c mice. *Infect Immun* **72**: 4668–4679.

Tomb, J.F.J., White, O.O., Kerlavage, A.R.A., Clayton, R.A.R., Sutton, G.G.G., Fleischmann, R.D.R., *et al.* (1997) The complete genome sequence of the gastric pathogen *Helicobacter pylori*. *Nature* **388**: 539–547.

Wadhams, G.H., and Armitage, J.P. (2004) Making sense of it all: bacterial chemotaxis. *Nat Rev Mol Cell Biol* **5**: 1024–1037.

Wang, H., and Matsumura, P. (1996) Characterization of the CheAS/CheZ complex: a specific interaction resulting in enhanced dephosphorylating activity on CheY-phosphate. *Mol Microbiol* **19**: 695–703.

Williams, S.M., Chen, Y.-T., Andermann, T.M., Carter, J.E., McGee, D.J., and Ottemann, K.M. (2007) *Helicobacter pylori* chemotaxis modulates inflammation and bacterium-gastric epithelium interactions in infected mice. *Infect Immun* **75**: 3747–3757.

Wolfe, A.J., and Berg, H.C. (1989) Migration of bacteria in semisolid agar. *Proc Natl Acad Sci USA* **86**: 6973–6977.

Wuichet, K., Alexander, R.P., and Zhulin, I.B. (2007) Comparative genomic and protein sequence analyses of a complex system controlling bacterial chemotaxis. *Meth Enzymol* **422**: 1–31.

Zhao, R., Collins, E.J., Bourret, R.B., and Silversmith, R.E. (2002) Structure and catalytic mechanism of the *E. coli* chemotaxis phosphatase CheZ. *Nat Struct Biol* **9**: 570–575.

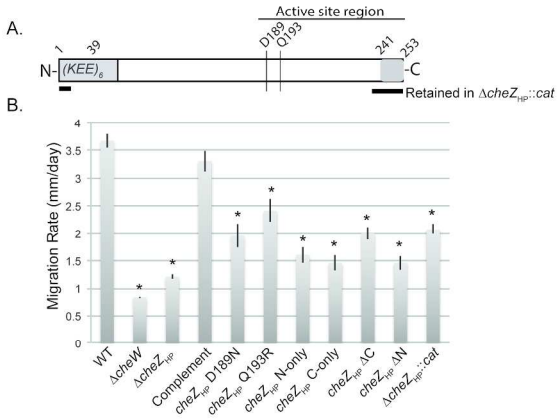

Figure 1. (A) Schematic of CheZHP protein. The active site region is indicated by a horizontal line above. The N terminal region (1-39) contains six copies of a highly charged amino acid se-quence (KEE). The active site residues are indicated by vertical lines (D189 and Q193R). The C terminal region (241-253) binds CheY-P. The portions retained in the original ΔcheZHP::cat al-lele are shown with thick horizontal lines below the CheZHP schematic. (B) Soft agar migration rates of H. pylori G27 wild type (WT), ΔcheW, and cheZHP isogenic mutants. Strains were stabbed into Brucella broth-FBS soft agar, and the diameter of the expanded colony measured after 4-5 days. The data represents the average of at least two biological replicates with at least three technical replicates. Error bars show standard error. * indicates significantly different from WT (P value <0.05) using Student's t test.
215x279mm (300 x 300 DPI)

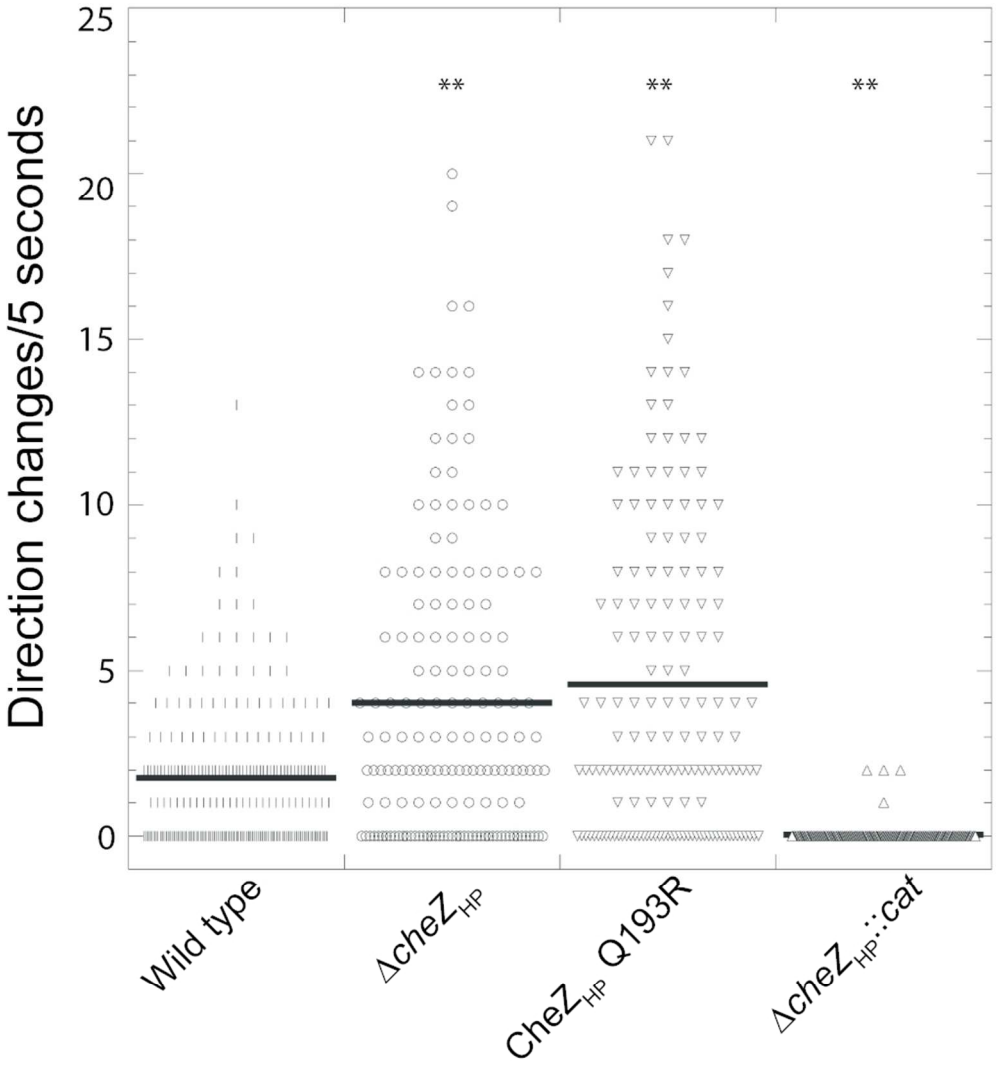

Figure 2. Swimming behavior of cheZHP mutant strains. H. pylori G27 cells in Brucella Broth with FBS (BB10) were filmed using microscopy, and then the number of directional changes in five seconds were counted. The number of examined cells (n) and average directional changes per cell (indicated by black solid lines) are as follow: WT (n = 230, 1.8), ΔcheZHP (n =156, 4.0), and cheZHP Q193R (n = 155, 4.6), cheZHP N-only (n=186, 7.4), ΔcheZHP::cat (n=211, 0.03). At least two biological replicates were used for each strain. ** indicates significantly different from wild type (P value <0.01) using Student's t test.
86x93mm (300 x 300 DPI)

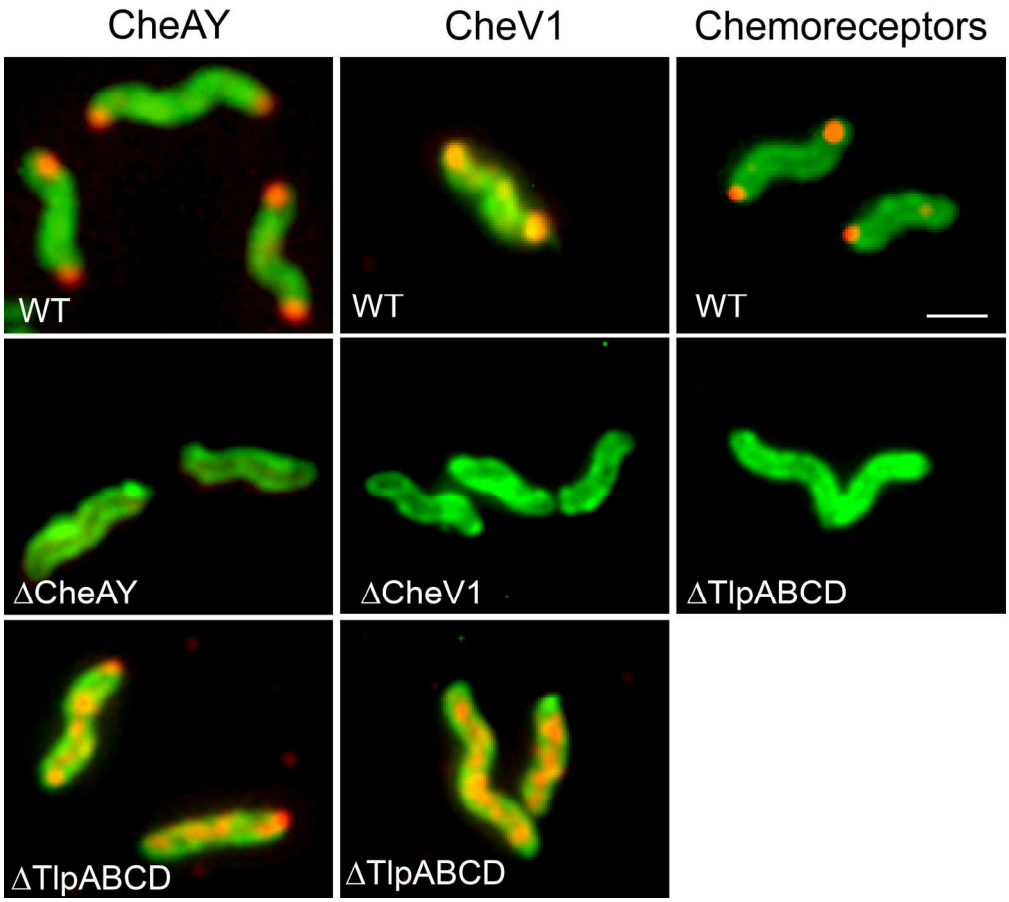

Figure 3. H. pylori chemoreceptors and core chemotaxis signaling proteins form a polar cluster anchored by the chemoreceptors. The protein examined is indicated across the top, and the strain backgrounds are indicated in white writing within each panel. CheAY, CheV1, and the chemo-receptors are shown in red, detected by immunofluorescence using rabbit polyclonal anti-CheAY, anti-CheV1, or anti-TlpA22 respectively, followed by incubation with anti-rabbit anti-bodies conjugated with Alexa Fluor® 594 to fluoresce red. H. pylori cells are green, visualized by chicken anti-H. pylori antibodies, followed by anti-chicken antibodies conjugated with Alexa Fluor® 488, to fluoresce green. Multiple bacteria are shown; in some cases these were captured from independent images.
173x157mm (300 x 300 DPI)

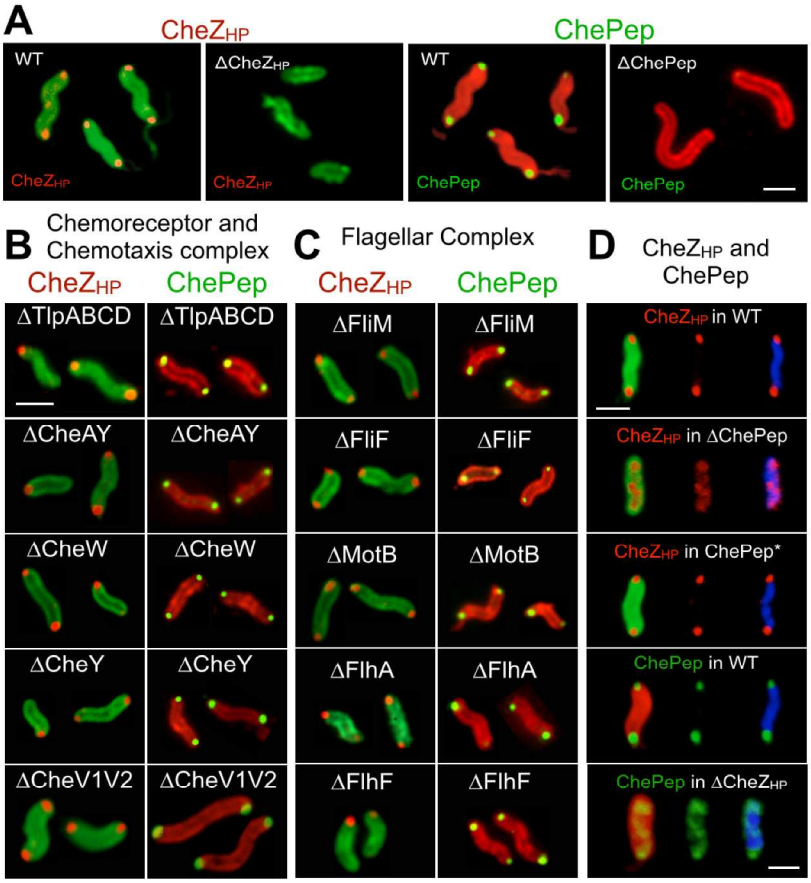

Figure 4. CheZHP and ChePep form a polar cluster that is independent from chemotaxis and fla-gellar-related proteins. Protein analyzed indicated above each set of relevant panels in a color matching the detection color. Strain background indicated in white writing within each panel. Multiple bacteria are shown for each mutant; in some cases these were captured from independ-ent images. Scale bar represents 1 μm. A. CheZHP (red) was detected using anti-CheZHP antibod-ies, followed by secondary antibodies conjugated to Alexa Fluor® 594 to fluoresce red. H. pylori cells (green) were visualized chicken anti-H. pylori antibodies, followed by secondary conjugat-ed with Alexa Fluor® 488. B. CheZHP and ChePep localization in chemotaxis signaling mutants. CheZHP (red) was visualized as in Panel A. ChePep (green) was visualized using anti-ChePep antibodies, followed by secondary anti-rabbit antibodies conjugated to Alexa Fluor 488, while whole bacteria were visualized using chicken anti-H. pylori followed by secondary antibodies conjugated to Alexa Fluor 594 to fluoresce red. C. CheZHP and ChePep localization in flagellar mutants. CheZHP and ChePep visualized as in Panel A and B, respectively. D. CheZHP and ChePep are mutually dependent on each other. CheZHP and ChePep visualized as in Panel A and B, respectively, with the addition

of cells being visualized by DAPI DNA staining (blue).
361x529mm (300 x 300 DPI)

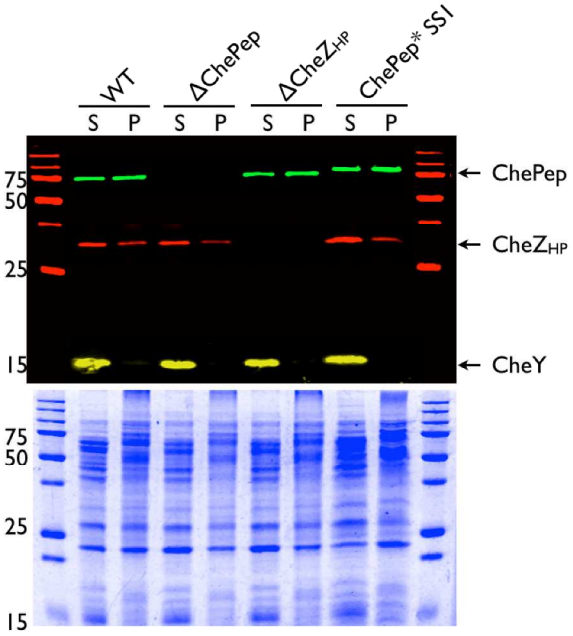

Figure 5. ChePep and CheZHP are expressed independently of each other. Western blot analysis of 8-16% gradient gels of ChePep, CheZHP and CheY association with triton-insoluble (Pellet, P) and soluble fractions (S). The bottom panel shows coomassie stained identical sam-ples. Molecular weight in kilodaltons indicated at the left of each panel. The predicted molecular weight of ChePep is 56 kilodaltons, but it migrates slower in SDS-PAGE presumably due to its high charge.
361x529mm (300 x 300 DPI)

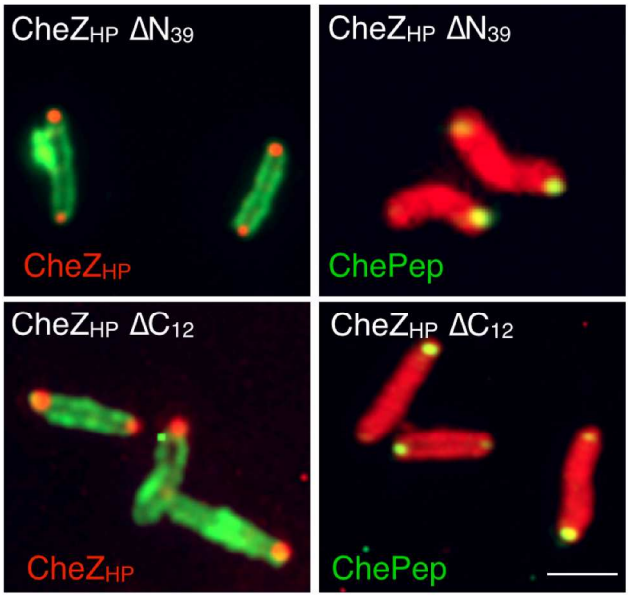

Figure 6. CheZHP N and C termini are dispensable for polar localization of CheZHP (left panels, red) and ChePep (right panels, green). CheZHP and ChePep were detected by immunofluores-cence as described in Fig. 4. Protein analyzed indicated in each set of relevant panels in a color matching the detection color. Strain background indicated in white writing within each panel. Multiple bacteria are shown; in some cases these were captured from independent images.
361x529mm (300 x 300 DPI)

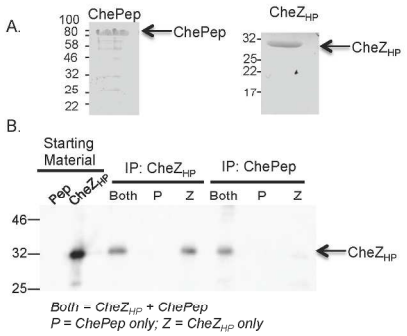

Figure 7. CheZHP and ChePep interact directly. A. Coomassie-stained SDS-PAGE gel of puri-fied ChePep (left) and CheZHP (right) proteins. Molecular weight in kilodaltons indicated at the left of each panel. B. Co-immunoprecipitation of CheZHP and ChePep, analyzed by western blot-ting of 10% SDS-PAGE gels with anti-CheZHP. From left to right: (1) Pep: the ChePep starting material (2) CheZHP: the CheZHP starting materials; (3-5) Immunoprecipitation (IP) with anti-CheZHP, incubated with a mixture of ChePep+CheZHP (both), ChePep (P) or CheZHP (Z); (6-8) IP with anti-ChePep, incubated with each set of proteins as in (3-5). The positions of ChePep and CheZHP are indicated on the right.
254x190mm (300 x 300 DPI)

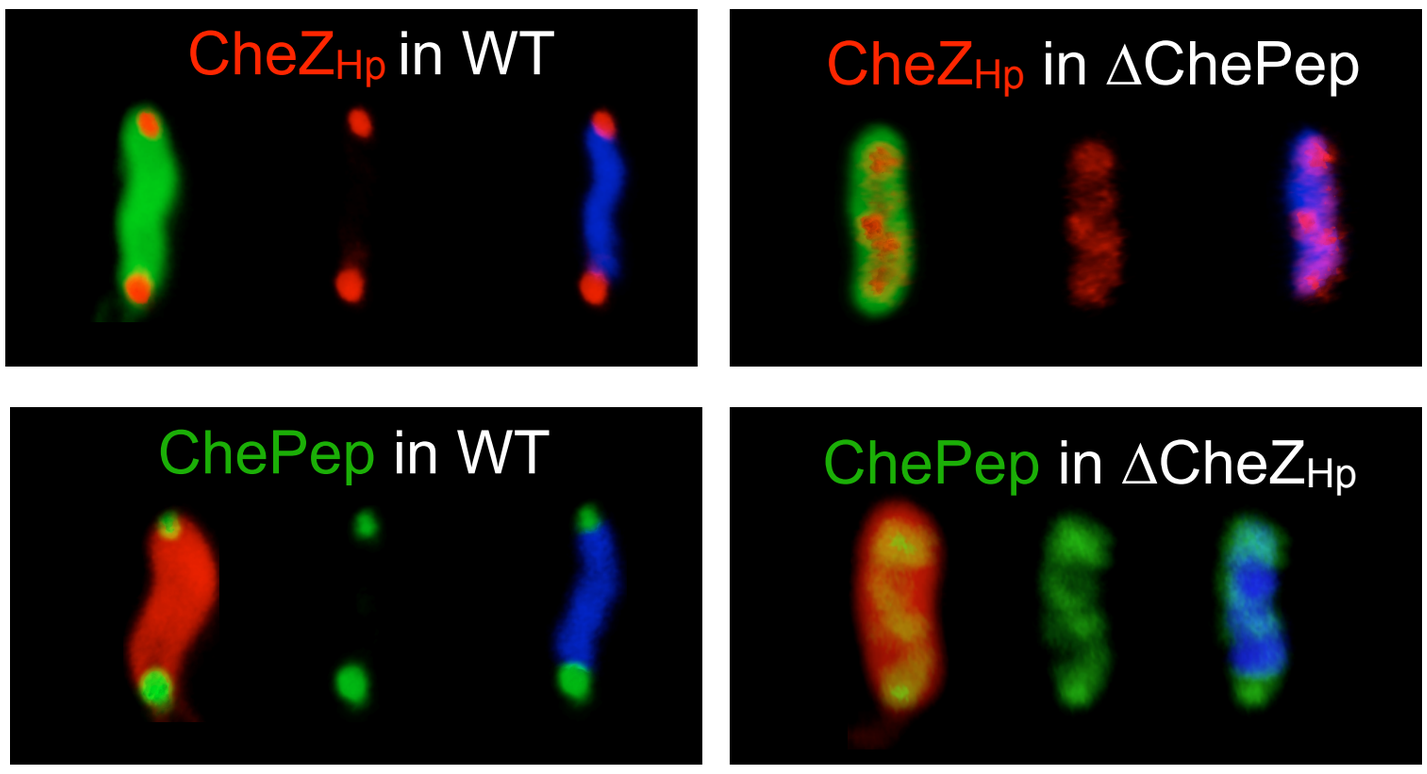
CheZHp in WT
CheZHp in ΔChePep
ChePep in WT
ChePep in ΔCheZHp

Chemotaxis phosphatases such as CheZ localize to specific cellular sites to provide optimal chemotaxis performance. We show here that phosphatases exploit unexpected locations beyond the flagellar and chemoreceptor complexes. Specifically, the CheZ phosphatase of *Helicobacter pylori* localizes independent of the motility and chemoreceptor proteins, and instead relies on interactions with the ChePep chemotaxis protein. Localizing some chemotaxis proteins separate from the canonical motility and chemotaxis complexes may be a mechanism to provide unique regulatory inputs to CheZ and ChePep.